Investigation of generation of the $\frac{3}{2}\omega_0$ harmonic produced by spherical laser irradiation of a plasma

N. G. Basov, V. Yu. Bychenkov, A. A. Zozulya, M. O. Kochevoĭ, M. V. Osipov, A. A. Rupasov, V. P. Silin, G. V. Sklizkov, V. T. Tikhonchuk, D. V. Shanditsev, and A. S. Shikanov

P. N. Lebedev Institute, USSR Academy of Sciences
(Submitted 24 December 1986)
Zh. Eksp. Teor. Fiz. **92**, 1700–1713 (May 1987)

Radiation generated by a laser plasma at the frequency of the $\frac{3}{2}\omega_0$ harmonic was investigated in experiments on heating of spherical shell targets. A theoretical analysis was carried out of the influence on the spectral characteristics of this radiation, as well as on the electron temperature in the $n_c/4$ region, by the following factors: wave damping in the plasma, oblique incidence of the heating radiation on the plasma, the presence of spontaneous magnetic field, velocity of the $n_c/4$ region, and the velocity of the matter in the corona. It is shown that the latter plays a dominant role in the shift of the blue component of the $\frac{3}{2}\omega_0$ harmonic, making it possible to interpret the experimental results.

1. INTRODUCTION

One of the most important tasks in research into laser thermonuclear fusion is optimization of the coupling between the laser and the plasma it produces. This calls for obtaining, in the course of the experiment, detailed information on the parameters of just that part of the laser-plasma corona in which the heating radiation is absorbed. The most suitable way of achieving this is to record the laser-plasma emission in the optical band, especially harmonics having the heating-radiation frequency ω_0.

The possibilities of measuring the laser-plasma parameters by spectral measurements of the second harmonic of the heating-radiation frequency were verified and indicated in a review by Basov *et al.*[1] on the basis of an analysis of a large group of theoretical and experimental studies. Another region of importance for interaction between laser radiation and a plasma is one having a density one-fourth the critical value n_c. It can be investigated by using plasma at frequencies of half-integer harmonics of laser radiation.

The first indications of feasibility of diagnostics of plasma parameters and of plasma turbulence in the region of one-quarter of the critical density, using the spectrum of the $\frac{3}{2}\omega_0$ harmonic (ω_0 is the frequency of the heating radiation), are contained in Refs. 2–4. The method proposed in these papers of determining the local electron temperature is connected with the characteristic two-component structure of the $(\frac{3}{2}\omega_0)$-harmonic spectrum. This method found qualitative confirmation in a large number of experiments[2,3,5–25] which revealed, at the same time, a number of disparities between the experimental data and the predictions of the simplest theoretical model[3,4] (see also Ref. 26). We note among these disparities is an overestimate of the electron temperature (by an approximate factor 1.5–2), obtained from measurements of the spectrum of the $\frac{3}{2}\omega_0$ harmonic, are compared with the data of other procedures,[3,11–15,20,21] a difference between the intensities of the doublet of the $\frac{3}{2}\omega_0$ harmonic,[2,3,6,9–15,19,20] and a dependence of the splitting of the $(\frac{3}{2}\omega_0)$-harmonic spectrum on the angle of its emission from the plasma.[12–14] In addition, in some experiments the spectrum of the $\frac{3}{2}\omega_0$ harmonic had not two components, but either only one[22] or more than two.[25]

All this has called for a more profound development of the theoretical premises concerning the laws governing the generation of half-integer harmonics. The simplest theoretical model of a uniform plasma layer[2–4,26] was previously generalized to allow for an inhomogeneous plasma density,[12,27] for oblique incidence of laser radiation, and for polarization of the latter.[28–30] To analyze the experiments it is necessary also to take into account a large group of effects, such as plasma expansion, its motion as a whole (e.g., on account of compression of a shell target) during the action of a laser pulse,[31] nonlinear interaction, damping of plasma waves, and spontaneous magnetic fields.[32,33]

According to contemporary notions, generation of half-integer harmonics in a plasma produced by laser radiation is due to two-plasmon parametric instability, i.e., to the decay of the incident transverse electromagnetic wave (photon) into two longitudinal plasma waves (plasmons) having frequencies approximately equal to half the pump-wave frequency. This process takes place in a plasma region of density close to one-quarter critical, where the frequency ω_0 is close to double the Langmuir frequency ω_{Le}. Since the incident electromagnetic wave carries momentum, the momenta of the excited plasma waves, and hence their frequencies, differ from one another. The plasma motion, by virtue of the Doppler effect, leads also to a frequency shift of the excited waves.

The generation of the $\frac{3}{2}\omega_0$ harmonic is due to coalescence of the plasma waves excited in two-plasmon decay, on the one hand, and the heating radiation, on the other. The spectrum of the $\frac{3}{2}\omega_0$ harmonic is determined by the spectrum of the plasma oscillations in the coalescence region. This spectrum, generally speaking, can differ from the spectrum of the excited wave, since the regions of the coalescence and of the two-plasmon decay are spatially separated. In the simplest case of normal incidence of the pump wave on an inhomogeneous plasma at rest, the spectrum of the harmonic has two components with equal and symmetrically located satellites relative to the nominal value.[27] Damping of the plasma waves leads to a difference between the intensities of the spectral components, while the nonlinear interaction of the plasma waves can lead to an increase of the number of the components (see, e.g., Ref. 25). Oblique incidence and

 0038-5646/87/050954-08$04.00

spreading of the plasma lead to asymmetric locations of the components relative to the value $\frac{3}{2}\omega_0$.

We report below the results of an analysis of the effect of various factors on the form of the spectrum of the $\frac{3}{2}\omega_0$ harmonic. We interpret on the basis of this investigation the experimental data on heating of spherical shell targets in the "Del'fin-1" laser installations. We show that the shifts of the components in the spectrum of the $\frac{3}{2}\omega_0$ harmonic agree qualitatively with the theoretical premises based on their dependences on the electron temperature and on the rate of plasma expansion in a density region close to one-quarter the critical value.

2. RESULTS OF THEORETICAL ANALYSIS OF GENERATION OF THE HARMONIC IN A LASER PLASMA

2.1. We demonstrate the effect of damping of plasma and electromagnetic waves on the form of the harmonic spectrum first for the simplest case of normal incidence of the pump wave on a plane-layered plasma having a density that increases monotonically along the x axis. In the vicinity of one-quarter critical density, owing to two-plasmon decay, plasma waves are produced with frequencies ω_l and $\omega_0 - \omega_l$ and having wave-vector components $\mathbf{k}_{l\perp}$ and $-\mathbf{k}_{l\perp}$ perpendicular respectively to the density gradient. The position of the decay point $x_r(\omega_l, \mathbf{k}_{l\perp})$ on the density profile is determined by the momentum conservation law $k_{lx}(\omega_l, \mathbf{k}_{l\perp}) + k_{lx}(\omega_0 - \omega_l, -\mathbf{k}_{l\perp}) = k_0$, from which follows

$$k_{lx}(x_r) = 4(\omega_l - \omega_0/2)\,(3\omega_0 r_{De}^2 k_0)^{-1} + k_0/2,$$

where $k_0 = 3^{1/2}\omega_0/2c$ is the pump wave number in the region of quarter-critical density, r_{De} is the Debye radius, and c is the speed of light. The waves considered are amplified in the vicinity of the point x_r exponentially, with a gain $\varkappa(\omega_l, \mathbf{k}_{l\perp})$.

When the longitudinal waves that are the products of two-plasmon decay propagate in the plasma, the x components of their wave vectors change. These waves can therefore land also in plasma regions in which the following condition for coalescence of Langmuir waves with the pump wave is met:

$$k_{lx}(x_\pm) + k_0 = \mp k_{\eta_2 x} = \pm(\omega_0/2c)\,(8 - 9\sin^2\theta)^{1/2}.$$

Here θ is the angle of emergence of the $\frac{3}{2}\omega_0$ harmonic emission, and the $\pm$ signs correspond either to generation of a harmonic that propagates into the interior of the plasma ($+$) and emerges subsequently into the vacuum after reflection from the dense layer, or to generation of a harmonic in the direction of decreasing plasma density ($-$). The frequency of the harmonic is equal to the sum of the frequencies of the pump and Langmuir waves: $\omega = \omega_l + \omega_0 \approx \frac{3}{2}\omega_0$.

According to Ref. 27, the gain $\varkappa$ has two identical maxima $\varkappa = \varkappa_{\max} = (v_E/v_{Te})^2 k_0 L/24$, where v_E is the amplitude of the electron-oscillation velocity in the region of the quarter critical density, v_{Te} is the thermal velocity of the electrons, and L is the inhomogeneity scale. Accordingly, the spectrum of the harmonic also has two maxima of equal intensity at the frequency values

$$\Delta\omega = \omega - {}^3/_2\omega_0 = \pm {}^9/_8\omega_0 (v_{Te}/c)^2 (1 + 12\sin^2\theta)^{1/2}. \qquad (1)$$

In the presence of wave damping, the intensity of the $\frac{3}{2}\omega_0$ harmonic is proportional to $\exp(2\pi\varkappa - \tau)$, where $\tau = \tau_l + \tau_{3/2}$ is the sum of the absorption coefficient of the plasma waves between the decay and coalescence points (τ_l) and the absorption coefficient of the harmonic along the path from the coalescence point to the emergence to the vacuum ($\tau_{3/2}$). In the case of an exponential density profile $n_e(x) \propto \exp(x/L)$ and a uniform temperature distribution

$$\tau_{\eta_2} = (\nu L/c) f(\theta),$$

where ν is the frequency of the electron collisions in the quarter-critical-density region, we have

$$f = f_2(\theta) = 2[\cos\theta - (\cos^2\theta - {}^1/_9)^{1/2}] \times [{}^1/_3 + 3\cos^2\theta - \cos\theta\,(9\cos^2\theta - 1)^{1/2}],$$

if the harmonic propagates from the coalescence region into the vacuum, and

$$f = f_1(\theta) = 6\cos^2\theta[(9\cos^2\theta - 1)^{1/2} + \cos\theta],$$

if the harmonic propagates from the coalescence region first into the interior of the plasma to the reflection surface, and then back to the vacuum.

The damping of the Langmuir waves along the path from the region of their excitation to the coalescence region is equal to

$$\tau_l = (\nu L/c)\Phi,$$

where

$$\Phi = \Phi_1(\theta) = 3^{1/2}[3 + (1 + 12\sin^2\theta)^{1/2} - 2(8 - 9\sin^2\theta)^{1/2}],$$

if a "blue" satellite ($\omega > \frac{3}{2}\omega_0$) traveling into the interior is excited in the coalescence region. In the case of excitation of a harmonic that travels out of the plasma we have

$$\Phi = \Phi_2(\theta) = 3^{1/2}[3 + (1 + 12\sin^2\theta)^{1/2} + 2(8 - 9\sin^2\theta)^{1/2}]$$

for the blue satellite and

$$\Phi = \Phi_3(\theta) = 3^{1/2}[3 - (1 + 12\sin^2\theta)^{1/2} + 2(8 - 9\sin^2\theta)^{1/2}]$$

for the "red" satellite.

The damping of the blue satellite in the spectrum of the $\frac{3}{2}\omega_0$ harmonic is thus different from that of the red one. The blue satellites can be produced in two ways. First, by coalescence of the pump wave with the Langmuir wave produced via two-plasmon decay of a Langmuir wave. The resultant electromagnetic wave propagates then into the interior of the plasma and emerges after reflection from the denser layers. Its absorption coefficient is

$$\tau = \tau_{B_1} = (\nu L/c)\Psi_1, \quad \Psi_1 = \Phi_1 + f_1.$$

Second, the blue satellite appears when the pump wave coalesces with the reflected Langmuir wave. The harmonic emerges then to the outside and

$$\tau = \tau_{B_2} = (\nu L/c)\Psi_2, \quad \Psi_2 = \Phi_2 + f_2.$$

No wave reflection takes place when the red satellite is generated, so that

$$\tau = \tau_R = (\nu L/c)\Psi_3, \quad \Psi_3 = \Phi_3 + f_2.$$

The intensity ratio of the red and blue satellites in the spectrum of the $\frac{3}{2}\omega_0$ harmonic is equal to $I_R/I_B = \exp(\tau - \tau)$, where $\tau_B = \min(\tau_{B1}, \tau_{B2})$. Plots of $\Psi_{1,2,3}(\theta)$ are shown in

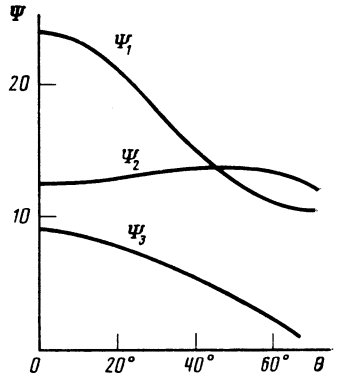

FIG. 1. Absorption coefficients of the blue ($\Psi_{1,2}$) and red (Ψ_3) components in the spectrum of the $\frac{3}{2}\omega_0$ harmonic vs the emission angle θ at normal incidence of the pump wave.

Fig. 1, from which it follows that the damping of the blue satellite exceeds that of the red one, i.e., $I_R > I_B$. It is also evident from this figure that at angles $\theta < 45°$ generation of a blue satellite is favored, with direct emission into the vacuum ($\Psi_1 > \Psi_2$) i.e., at $\theta < 45°$ the reflection of the harmonic from the dense plasma layer does not influence substantially the form of its spectrum.

2.2. Oblique incidence of the pump wave is another cause of the difference between the satellite intensities of the satellites in the spectrum of the $\frac{3}{2}\omega_0$ harmonic. According to Ref. 28, the coefficient of convective amplification is determined in this case by the expression

$$\varkappa = \frac{(\mathbf{k}_r\mathbf{v}_E)^2(\mathbf{k}_r\mathbf{k}_0 - k_0^2/2)^2 L}{6v_{T_e}^2 k_{0x}\mathbf{k}_r^2(\mathbf{k}_r - \mathbf{k}_0)^2}, \qquad (2)$$

where $\mathbf{k}_0 = (k_{0x}, \mathbf{k}_{0\perp})$ is the wave vector of the pump wave,

$$k_{0x} = (\omega_0/c)(^3/_4 - \sin^2\theta_0)^{1/2}, \quad k_{0\perp} = (\omega_0/c)\sin\theta_0,$$

$\mathbf{k}_r = (k_{lx}(x_r), \mathbf{k}_{l\perp})$ is the wave vector of the plasma wave at the decay point $x = x_r$,

$$k_{lx}(x_r) = \frac{\omega_0(\omega_l - \omega_0/2)}{3v_{T_e}^2 k_{0x}} - \frac{(\mathbf{k}_{0\perp}, \mathbf{k}_{l\perp} - \mathbf{k}_{0\perp}/2)}{k_{0x}} + \frac{k_{0x}}{2}. \qquad (3)$$

Equations (2) and (3) allow us to calculate the form of the $\frac{3}{2}\omega_0$ harmonic spectrum, given the polarization of the pump wave and the direction of observation of the harmonic.[28–30] In the case of an s-polarized pump wave the satellites are symmetrically shifted in the red and blue directions relative to the value of $\frac{3}{2}\omega_0$. If the incidence is not normal, however, the intensities of the red and blue satellites differ already even in the absence of damping, and at $\mathbf{k}_{0\perp}\cdot\mathbf{k}_{3/2\perp} < \frac{3}{2}k_{0\perp}^2$, in the majority of solid angles, the intensity of the red satellite is higher than that of the blue one, as is usually observed in experiment. For a p-polarized pump wave, the shifts of the red and blue satellites are unequal; moreover, the number of components in the spectrum of the harmonic can exceed two.[28]

2.3. The spectral shift of the satellites can also be influenced by the motion of the corona and the plasma flux through the quarter-critical density region. Let U denote the velocity of this region as a result of compression of a spherical target. The presence of U leads to a Doppler shift of the spectrum of the harmonic by an amount $\delta\omega = U(k_{3/2x} - k_{0x})$ relative to the $\frac{3}{2}\omega_0$ spectrum position corresponding to $U = 0$. Estimates show that at typical corona velocities $U \approx 5\cdot 10^6$ cm/s in the quarter-critical-density region and at an electron temperature $T_e \approx 1$ keV the Doppler shift $\delta\omega$ ranges from one to ten percent of the distance between the components in the spectrum of the $\frac{3}{2}\omega_0$ harmonic. A stronger influence on the spectral distribution of the harmonic is exerted by the flow-through of the plasma through the quarter-kinetic-density region (plasma expansion).[31] Let u be the rate of flow of the plasma relative to this region. Calculation of the gain, with allowance for plasma flow at a velocity u is similar to the one calculated at $u = 0$ in Refs. 28 and 29 and yields for the gain the expression (2) in which $k_{lx}(x_r)$ should be expressed not by (3) but by the expression

$$k_{lx}(x_r) = \left(1 - \frac{\omega_0 u}{3k_{0x}v_{T_e}^2}\right) \times \left[\frac{\omega_0(\omega_l - \omega_0/2)}{3k_{0x}v_{T_e}^2} - \frac{(\mathbf{k}_{0\perp}, \mathbf{k}_{l\perp} - \mathbf{k}_{0\perp}/2)}{k_{0x}}\right] + \frac{k_{0x}}{2}. \qquad (4)$$

It follows from a comparison of (3) and (4) that the plasma expansion leads to a change of the frequency shift in the spectrum of the harmonic in accordance with the law

$$\Delta\omega = \omega - \frac{3}{2}\omega_0 = \pm\left(1 - \frac{\omega_0 u}{3k_{0x}v_{T_e}^2}\right)\cdot\frac{9}{8}\left(\frac{v_{T_e}}{c}\right)^2\omega_0 \times\left[\left(1 - \frac{4}{3}\sin^2\theta_0\right)(1 + 12\sin^2\theta\sin^2\varphi) + 12(\sin\theta\cos\varphi - \sin\theta_0)^2\right]^{1/2} + \frac{u}{k_{0x}}\left(\mathbf{k}_\perp\mathbf{k}_{0\perp} + \frac{3}{2}k_{0\perp}^2\right), \qquad (5)$$

i.e., the expansion leads to an additional satellite shift amounting to $(u/k_{0x})(\mathbf{k}_\perp\cdot\mathbf{k}_{0\perp} - \frac{3}{2}k_{0\perp}^2)$ and to a decrease of the distance between them by a factor $(1 - \omega_0 u/3k_{0x}v_{Te}^2)$. The parameter $\mathbf{k}_\perp\cdot\mathbf{k}_{0\perp} - \frac{3}{2}k_{0\perp}^2$, which determines the shift of the spectra, is equal to the parameter that determines the relative intensity of the satellites in the spectrum of the harmonic in the case of oblique incidence of an s-polarized pump wave. As indicated above, for most harmonic-emission directions this parameter is negative. The intensity of the red satellite exceeds therefore that of the blue one, and the entire spectrum as a whole is shifted towards the red. For typical plasma-corona conditions, when the velocity u is approximately double that of sound, the shift of the spectrum of the harmonic is approximately 3–4 times smaller than the distance between satellites. This points to a connection between the asymmetry of the $\frac{3}{2}\omega_0$ harmonic spectrum and the plasma expansion.

2.4. We examine, finally, the influence of a quasistationary magnetic field on the form of the spectrum of the $\frac{3}{2}\omega_0$ harmonic. Several authors[32,33] attributed the two-component structure of the spectrum of the harmonic to the influence of the magnetic field. The quasistationary magnetic fields recorded in a laser plasma are of the order of $B \leqslant 1$ MG, corresponding to an electron-cyclotron frequency $\Omega = eB/mc \lesssim 2\cdot 10^{13}\ \mathrm{s}^{-1}$. This is lower by about two orders than the laser-emission frequency. Under the condition $\Omega \ll \omega_0$, two-plasmon parametric instability corresponds to decay of the pump wave into two upper-hybrid oscillations with a dispersion law

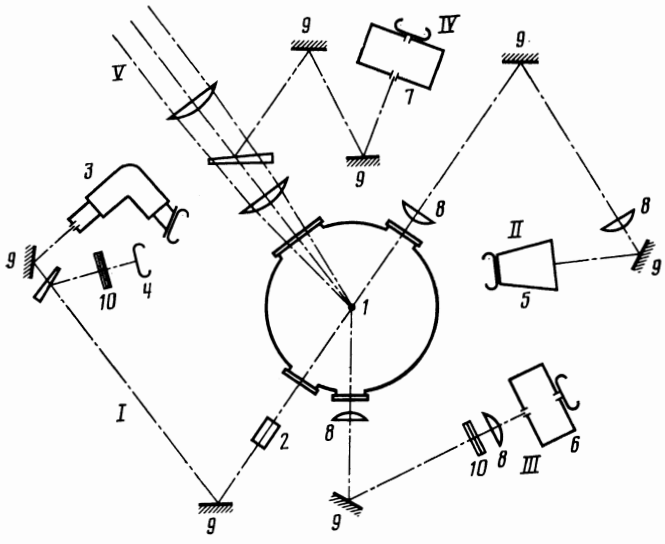

FIG. 2. Diagram of experimental diagnostic apparatus: I, II, III, IV—registration channels; V—one of the composite heating beams; 1—chamber with target, 2—objective, 3—ISP-51 spectrograph, 4—photographic camera with set of light filters, 5—STE-1 spectrograph, 6 and 7—MDR-2 spectrograph, 8—lenses, 9—mirrors, 10—light filters.

$$\omega_l(\mathbf{k}) = \omega_{Le} + {}^1/_2(\Omega^2/\omega_{Le})\sin^2\chi + {}^3/_2 k^2 v_{Te}^2/\omega_{Le}, \qquad (6)$$

where $\omega_{Le} \approx \omega_0/2$, and χ is the angle between the wave vector $\mathbf{k}$ of the Langmuir wave and the magnetic field. In accordance with (6), the magnetic field leads to an additional frequency shift in the spectrum of the $\frac{3}{2}\omega_0$ harmonic, by an amount $\sim\Omega^2/\omega_0$. For $B\sim 1$ MG and $T_e \sim 1$ keV this is smaller by about two orders than the temperature shift (1). Therefore, under typical conditions of a laser plasma, a magnetic field exerts a weak influence on the spectra of the half-integer harmonics due to two-plasmon decay.

A much stronger influence on the decay-wave spectra is exerted by the magnetic field in stimulated Raman scattering (SRS). According to Ref. 33, frequency shifts of order $\sim\Omega$ can be produced in this case in the spectrum of the $\frac{1}{2}\omega_0$ harmonic. Estimates[14] show, however, that the SRS threshold in a laser plasma is much higher in the vicinity of the quarter-critical density than the threshold of the two-plasmon instability. There are therefore no grounds for attributing the wave emission from the quarter-critical-density region of a laser plasma to SRS process. Accordingly, the influence of the magnetic fields on the spectra of half-integer harmonics turns out to be a small effect.

3. INVESTIGATION OF THE SPATIAL AND SPECTRAL CHARACTERISTICS OF THE $\frac{3}{2}\omega_0$ HARMONIC EMISSION IN THE "DEL'FIN-1" INSTALLATION

3.1. The experiments on heating spherical shell targets were performed with the "Del'fin-1" installation. Six laser beams, each consisting of 18 beams of 45 mm diameter, were focused on a spherical glass target of diameter $2R_0 = 400$–$850\,\mu$m with wall thickness $\Delta R_0 = 0.76$–$2.85\,\mu$m. The energy on the target surface ranged from 0.5 to 1.2 kJ, the pulse duration was 2.5–4.5 ns (at half-intensity level), the energy flux density on the target surface reached 10^{14} W/cm^2, and the width of the incident-radiation spectrum was $\Delta\lambda_0 \approx 40$ Å.

The scattered radiation was investigated in several registration channels (Fig. 2). In the first channel, the target image magnified 100 times was projected on the slit of an ISP-51 prism spectrograph 3. The spatial resolution in this channel was 20 μm. In the second channel the target image was projected on the slit of STE-1 spectrograph 5 with inverse dispersion ~ 12.8 Å/mm in the $\frac{3}{2}\lambda_0$ wavelength region. The direction of the second channel was diametrically opposed to that of the first. In both channels it was possible to record simultaneously the emission spectra of the plasma in a wide spectral range including the frequencies $\omega_0 > \frac{3}{2}\omega_0$ and $2\omega_0$. The spatial resolution in the first channel was high at moderate spectral resolution, while the second channel ensured high spectral resolution for registration integral over the target. In addition, the scattered radiation was recorded in the third channel with an MDR-2 spectrograph 6 having an inverse dispersion 40 Å/mm. The first registration channel included also a system that permitted two-dimensional photography of the plasma in emission close to the $\frac{3}{2}\omega_0$ harmonic, as separated with a set of light filters 4. The spectrum of the heating radiation was measured in one of the laser beams with the aid of MDR-2 spectrograph 7.

To clarify the target-irradiation geometry and the registration of the spectrograms with spatial resolution, Fig. 3 shows the arrangement of the heating beams and of the spec-

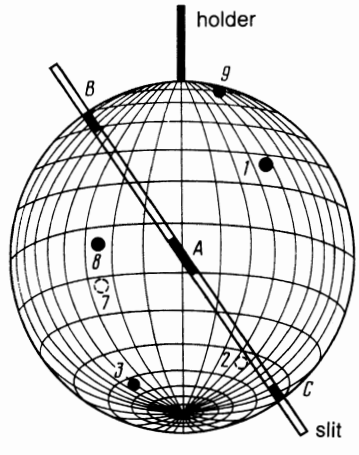

FIG. 3. Arrangement of heating beams and of spectrograph in target image for the first registration channel with spatial resolution. The axes of the heating beam are marked by numbered circles.

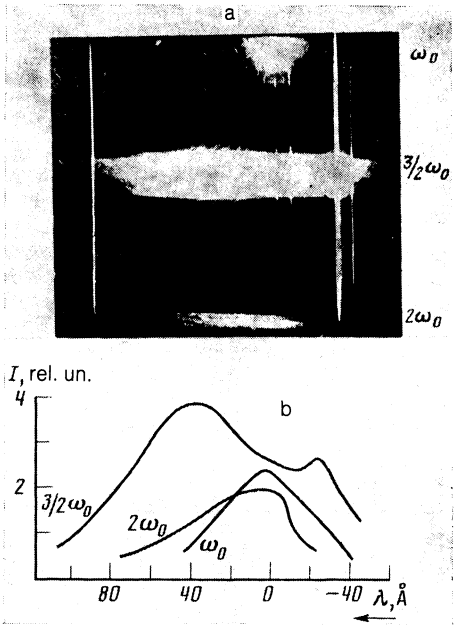

FIG. 4. Spectrograms (a) and spectral distributions of intensity (b) of plasma emission at the frequencies ω_0, $\frac{3}{2}\omega_0$, and $2\omega_0$, obtained in the second registration channel for a glass target of diameter $2R_0 = 490.7\ \mu$m and wall thickness $\Delta R_0 = 1.3\ \mu$m.

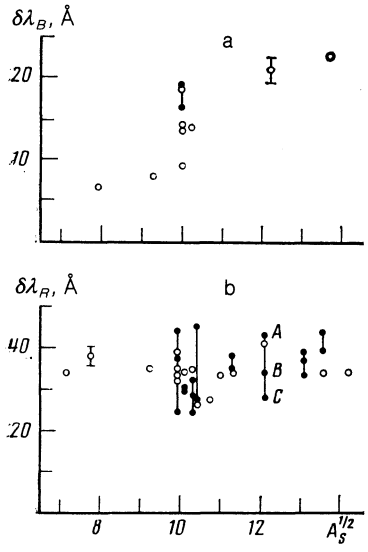

FIG. 5. Shifts of the blue ($\delta\lambda_B$, a) and red ($\delta\lambda_R$, b) components of the $\frac{3}{2}\omega_0$ harmonic for shell targets with different aspect ratios $A_S = R_0/\Delta R_0$. The light circles show the values obtained in the second channel, and the dark ones (joined by segments) in the first registration channel with spatial resolution.

trograph slit over the target image for the first registration channel. The axes of the heating beams are marked by numbered circles, the dashed circles marking beams on the rear target surface as seen by the observer.

In all the observation directions, we registered in scattered radiation the $\frac{3}{2}\omega_0$ harmonic whose spectrum consisted of two components: red, shifted towards longer wavelengths relative to the exact value $\frac{2}{3}\lambda_0$, and blue, shifted in the opposite direction.

Figure 4 shows typical spectrograms of the scattered radiation at the fundamental frequency ω_0 and at the harmonics $\frac{3}{2}\omega_0$ and $2\omega_0$, obtained in the second observation channel in one of the experiments. The emissions at the frequencies ω_0, $\frac{3}{2}\omega_0$, and $2\omega_0$ were obtained respectively in the 2nd, 3rd, and 4th diffraction orders of the grating of the STE-1 spectrograph grating and could be simultaneously recorded by separating the orders.

It can be seen from Fig. 4 that the spectrum of the plasma-scattered radiation duplicates in the vicinity of the fundamental frequency the spectrum of the heating radiation and exhibits no noticeable displacement from the nominal value. Note that shifts smaller than 3 Å cannot be recorded because of the large width of the laser-emission spectrum. The similarity of the spectra of the heating radiation and that scattered at the fundamental frequency attests to the weak influence of nonlinear processes on the radiation reflection.

The second-harmonic spectrogram recorded in the second channel using infrared photographic film (to be able to record $\frac{3}{2}\omega_0$ and ω_0) has low photographic density, and one can see distinctly only its fundamental component due to the mechanism of linear transformation of the heating radiation into plasma oscillations (Fig. 4). One can also see an asymmetric broadening of the spectrum of the $2\omega_0$ harmonic towards the red, indicating that parametric instabilities make a certain contribution to its generation.[1]

The spectrum of the $\frac{3}{2}\omega_0$ harmonic in Fig. 4 shows clearly a two-component structure, the shifts of the red and blue components are $\delta\lambda_R = 34$ Å, $\delta\lambda_B = 23$ Å, and the width of the spectral distribution at half-maximum is ~ 113 Å, i.e., approximately three times wider than the incident-radiation spectrum; the component-intensity ratio at the maxima is 1.7.

Figure 5 shows the values of the shifts of the red and blue components in the spectrum of the $\frac{3}{2}\omega_0$ harmonic in the second registration channel (without spatial resolution—light circles) for targets with different aspect ratio $A_S = R_0/\Delta R_0$. The shift of the rad component varies little from experiment to experiment and amounts to $\delta\lambda_R \approx 30$–$40$ Å. At the same time, the shift of the blue component increases from 6 to 30 Å with increase of the aspect ratio (with decrease of the target-wall thickness) in the investigated range $50 < A_S < 200$.

The $\frac{3}{2}\omega_0$ harmonic spectrograms obtained with spatial resolution in the first channel reveal a dependence of the shift of the red component on the position of the harmonic-emission region on the target surface. Figure 6 shows one such spectrogram and the spectral distributions for different sections (A, B, C) of the target image. In accordance with the placement of the spectrograph slit on the target image (Fig. 3), the regions B and C on the spectrograms correspond to the edges of the target image, while region A corresponds to its central part. The shift of the red component for the central region A turns out, as a rule, to be larger than for the edge regions B and C (Figs. 5 and 6).

Using the spectrograms of the scattered radiation at the frequency $\frac{3}{2}\omega_0$ and at the fundamental frequency, obtained with spatial resolution in the first registration channel, one can obtain information on the dimensions of the plasma-corona regions that glow at these frequencies. Figure 7 shows the dimensions of these regions, referred to the initial target diameter, for shells with different aspect ratios. Since

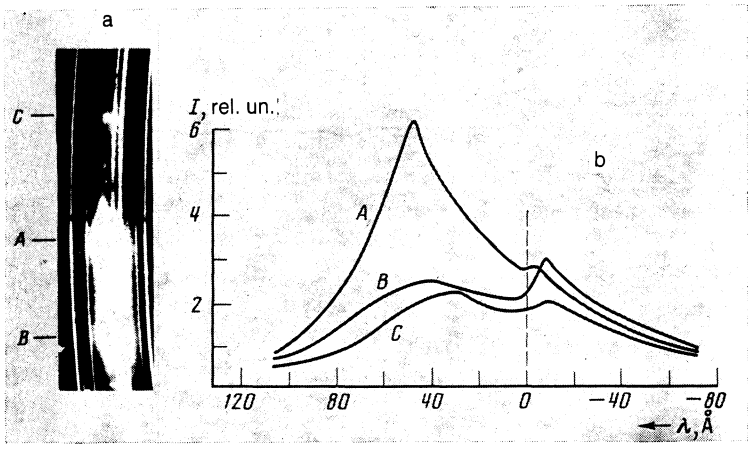

FIG. 6. Spectrogram of $\frac{3}{2}\omega_0$ harmonic (a) and spectral distributions (b) of the harmonic intensity for the central (A) and edge (B, C) regions of the plasma corona, as obtained in the first registration channel for a target of diameter $2R_0 = 602\ \mu$m and wall thickness $\Delta R_0 = 3\ \mu$m.

scattering at the frequency corresponds to the $n_c/4$ region, and scattering at $\frac{3}{2}\omega_0$ corresponds to a region with density $n_e \leqslant n_c$, it follows from Fig. 7 that for time-integrated registration of the scattered radiation the average diameter of the $n_c/4$ surface is $(1.0\text{–}1.5)2R_0$ for various targets, while the diameter of the n_c surface is less than $(0.7\text{–}1.0)2R_0$, in accord with the prevailing notions concerning the size of the plasma corona as obtained from hydrodynamic calculations.[34]

4. INTERPRETATION AND DISCUSSION OF EXPERIMENTAL RESULTS

To interpret the experimental results we have analyzed the influence exerted on the spectral-spatial characteristics of the $\frac{3}{2}\omega_0$ harmonic by all the factors considered in Sec. 2, as applied to the conditions of irradiation of shell targets in the "Del'fin-1" multichannel laser installation.

We have calculated the shapes of the spectra of the $\frac{3}{2}\omega_0$ harmonic with allowance of the influence of oblique propagation of the waves and of their damping. We considered an element of spherical plasma corona in the form of a one-dimensionally-inhomogeneous plasma slab with given scale of density inhomogeneity. The pump wave was assumed unpolarized and incident on the plasma at a given angle θ_0. Figure 8 shows the shapes of the spectra of the $\frac{3}{2}\omega_0$ harmonic emitted outward from the plasma in a direction defined by a polar angle θ and an azimuthal angle φ (angle between the pump-wave incidence plane and the harmonic-propagation plane). The damping was defined by the parameter

$$s = \frac{\nu(n_c/4)}{\omega_0}\left(\frac{v_{Te}}{v_E}\right)^2 \frac{24}{3^{1/2}\pi},$$

which is equal to the ratio of the length of spatial amplification of the Langmuir waves to their damping length. It is seen from Fig. 8 that the damping alters the relative intensity of the components in the spectrum of the harmonic, whereas their frequency shift depends weakly on the damping and on the difference between the pump-wave incidence angles, and allowance for these factors cannot explain the experimentally observed difference between the shifts of the red and blue components of the $\frac{3}{2}\omega_0$ harmonic.

Proceeding to discuss the influence of the plasma dynamics on the spectrum of the $\frac{3}{2}\omega_0$ harmonic, we note that hydrodynamic calculations and direct measurements yield a quarter-critical density-region velocity $U \lesssim 10^7$ cm/s. This can lead to a Doppler shift of the harmonic spectrum as a whole by up to 3–4 Å, whereas in experiment the half-differ-

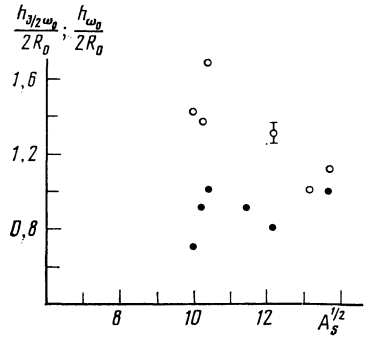

FIG. 7. Dimensions of regions of plasma emission at frequencies $\frac{3}{2}\omega_0$ and ω_0, referred to the initial target dimension, for targets with different aspect ratios. The light circles correspond to the $\frac{3}{2}\omega_0$ harmonic and to dark ones to scattered radiation at frequency ω_0.

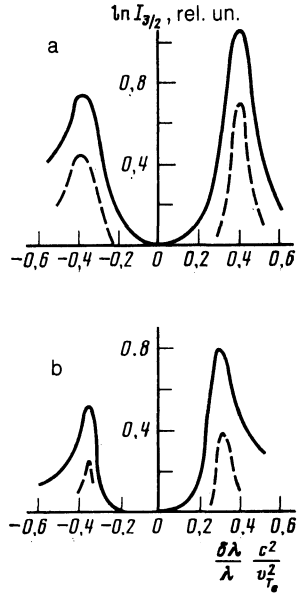

FIG. 8. Form of spectrum of $\frac{3}{2}\omega_0$ harmonic outgoing from the plasma in the direction $\theta = 20°$, $\varphi = 30°$ at a pump incidence angle $\theta_0 = 6°$ (a) and 20° (b) in the absence of collisions (solid lines and at $s = [\nu(n_c/4)\omega_0^{-1}](v_{Te}/v_E)^2(24/\pi\cdot 3^{1/2}) = 0.1$ (dashed).

TABLE I. Expressions for the shifts $\delta\lambda_R$ and $\delta\lambda_B$ for registration of the $\frac{3}{2}\omega_0$ harmonic integrated over the target (column 1) and with spatial resolution (columns 2–5). The angles are shown schematically in Fig. 9.

Designations of angles and shifts	1	2	3	4	5
θ_0	45°	45°	0	45°	45°
θ	45°	0	0 | 90°	90°	90°
φ	120°	No dependence on φ	No dependence on φ	0	180°
$\delta\lambda_R$	$40T-u$	$26T-0.6u$	–	$12T-0.4u$	$61T-1.3u$
$\delta\lambda_B$	$40T-8u$	$26T-5.4u$	–	$12T-2.4u$	$61T-13u$
$\delta\lambda_{R,B}$	–	–	$10.4T-0.7u$ | $10.4T-2.5u$	–	–

ence of the shifts of the red and blue components, i.e., the total shift of the spectrum, varies between 6 and 20 Å (Fig. 5). This difference of the shifts of the red and blue components can be attributed to leakage of the plasma through the $n_c/4$ region. This was shown in general form in Sec. 2. To analyze expression (5) for the shifts of the red and blue components under conditions of multibeam depolarized irradiation of a spherical target, we rewrite this expression in the form

$$\delta\lambda_{B,R}=10.4T\Phi-0.7u\frac{\Phi\pm4\sin\theta_0(\sin\theta_0-\sin\theta\cos\varphi)}{[1-{}^4/_3\sin^2\theta_0]^{1/2}}, \quad (7)$$

where

$$\Phi=[(1-{}^4/_3\sin^2\theta_0)(1+12\sin^2\theta\sin^2\varphi)$$
$$+12(\sin\theta_0-\cos\varphi\sin\theta)^2]^{1/2},$$

T is the electron temperature in the $n_c/4$ region in keV, u is the flow velocity of the plasma through the $n_c/4$ region in units of 10^7 cm/s, and $\delta\lambda$ is in Å. Under multibeam irradiation conditions, if the focal spot dimension is comparable with the target dimension, there exists a practically complete set of angles of heating radiation incident on the plasma, and for registration, integral over the target, of the spectra of the $\frac{3}{2}\omega_0$ harmonic (second observation channel), a part is played in the formation of the spectrogram by radiation with a large range of angles of outward motion of the harmonic from the plasma. It is therefore necessary to substitute in Eq. (7) in this case the mean values $\theta_0=45°$, $\theta=45°$, $\varphi=120°$, and the expressions for the shifts of the components take the form (see column 1 of Table I and Fig. 9)

$$\delta\lambda_R=40T-u, \quad \delta\lambda_B=40T-8u. \quad (8)$$

Hydrodynamic calculations[34] yield for u values $\sim(3-5)\cdot10^7$ cm/s, so that the influence of the expansion on the shift of the red component turns out to be small, within the experimental error. Since the value of $\delta\lambda_R$ is determined mainly by the plasma temperature, we get from (8) an estimated temperature $T\sim1$ keV. Note that the small scatter of the values of $\delta\lambda_R$ in a large number of target-surface-integrated measurements is evidence that the electron temperature averaged over the entire target surface is constant.

The blue-component shift depends much stronger on the rate of flow of the plasma through the $n_c/4$ region. It follows from a comparison of (8) with Fig. 5a that at an aspect ratio $A_S\sim50$ the value of u is $u_1\approx5\cdot10^7$ cm/s, and when A_S is increased to 200 the rate of expansion decreases to $u_2\approx3\cdot10^7$ cm/s. The relative velocity change $\Delta u=(u_1-u_2)/u_1$ needed to account for the experimental data is found to be relatively small, $\Delta u\approx0.4$, but the possibility of such a dependence of u on A_S at almost constant temperature is not obvious. Moreover, numerical calculations of the plasma-expansion dynamics for targets with different aspect ratios yield a considerably smaller value of Δu. The spectrograms discussed, however, were obtained in time-integrated measurements and in a number of cases the pulse duration exceeded the target-compression time. A substantial contribution to the recorded $\frac{3}{2}\omega_0$ harmonic spectrum can therefore be made by the instants of time after the target collapse, when the usual regime of mass consumption and flow rate no longer obtains. For high-aspect targets, the compression time is shorter than for low-aspect ones, since they are compressed at a higher rate. The instants of time after the target collapse can therefore be larger for such targets, meaning an effective decrease of the expansion rate of the mass with increase of the aspect ratio.

Registration of the $\frac{3}{2}\omega_0$ harmonic spectrum with spatial resolution over the target makes it possible to separate the radiation coming from different parts of the target and correspond to different angles of extraction of the harmonic from the plasma. Thus, for the central part of the plasma we have $\theta=0$ and Eq. (7) for the shifts of the harmonic components becomes independent of the angle φ between the pump-incidence and the harmonic-emission planes. For an average pump-incidence angle $\theta_0=45°$ we obtain then the expression (see column 2 in Table I):

$$\delta\lambda_R=26T-0.6u, \quad \delta\lambda_B=26T-5.4u. \quad (9)$$

Since these expressions are valid for all angles φ, it is preferable to record, for plasma-diagnostic purposes in the case of multibeam irradiation, the harmonic spectrum in the central part of the target, since Eqs. (9) yield simultaneously both the temperatures and expansion rates of the plasma. For the measured values $\delta\lambda_R=45$ Å and $\delta\lambda_B=15$ Å, which correspond to the spectrogram of Fig. 6, we obtain according to (9) the values $T=1.9$ keV and $u=6.2\cdot10^7$ cm/s.

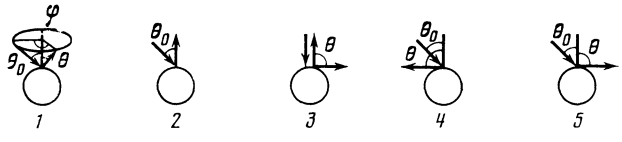

FIG. 9. Schematic representation of the angles θ_0, θ, and φ. The numbers correspond to the numbers of the columns in Table I.

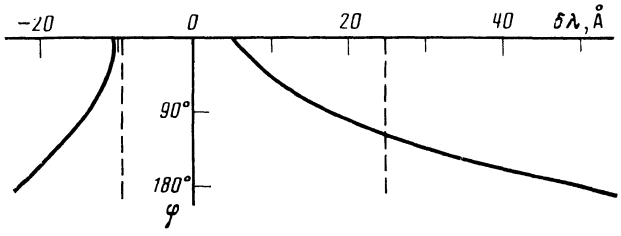

FIG. 10. Dependences of the shifts $\delta\lambda_R$ (left) and $\delta\lambda_B$ (right) on the angle φ between the pump-incidence plane and the plane of $\frac{3}{2}\omega_0$ emission at an incidence angle $\theta_0 = 45°$ and a harmonic-emission angle $\theta = 90°$ (registration of harmonic from the edge regions of the corona) at $T \approx 1$ keV and $u \approx 3 \cdot 10^7$ cm/s. The dashed straight lines correspond to the case $\theta_0 = 45°$ and $\theta = 0$ (registration of harmonic from the central region of the corona).

Note that $\delta\lambda_R$ and $\delta\lambda_B$ become independent of the angle φ also in the case $\theta_0 = 0$ (irradiation normal to the target surface) and for all harmonic emission angles θ (see column 3 in Table I). This case, however, is realized only for a small fraction of the heating radiation close to the axes of the heating beams (since the beam size is comparable with the target size), and is not decisive in the formation of the harmonic spectrum.

The situation for the $\frac{3}{2}\omega_0$ harmonic emission recorded from the edge regions of the plasma corona ($\theta = 90°$), the situation is made complicated by the fact that the expressions for $\delta\lambda_R$ and $\delta\lambda_B$ depend strongly on the angle φ. In particular, for the limiting values $\varphi = 0$ and 180° and for the average incidence angle $\theta_0 = 45°$ we obtain for the component shifts expressions in which the coefficients of T and u differ by several times (see columns 4 and 5 in Table I). Note that in this case the dependence on the shift angle φ is stronger for the red component than for the blue one, as follows from Fig. 10 plotted for $u = 3 \cdot 10^7$ cm/s and $T \sim 1$ keV.

The substantial difference between the expressions for the $\frac{3}{2}\omega_0$ harmonic component shifts, recorded in the central and edge parts of the corona, explains the spectrograms obtained with spatial resolutions. Thus, the dependence of $\delta\lambda_R$ and $\delta\lambda_B$ on φ in the case of the edge regions of the corona smoothens the peak of the red component of the harmonic for these regions (B and C of Fig. 6) compared with the central region (A, Fig. 6). The observed excess of the $\delta\lambda_R$ shift for the central region of the corona over $\delta\lambda_B$ for the edge regions is evidence that the largest contribution to the recorded spectrum of the harmonic from the edge region is made by the harmonic emission corresponding to small angles $\varphi < 100°$ (see Fig. 10).

5. CONCLUSION

We have investigated the laws governing the emission of the $\frac{3}{2}\omega_0$ harmonic in multibeam heating of spherical shell targets by neodymium-laser radiation of energy ~ 1 kJ, and reported the main harmonic-generation-theory results based on the mechanism of Raman scattering of the heating radiation by plasma waves excited in the vicinity of the quarter-critical density on account of two-plasmon parametric instability. The harmonic-radiation spectrum has as a rule two components, with the spectral shifts of the components proportional to the plasma temperature and dependent also on the rate of flow of the plasma through the $n_c/4$ region and on the incidence angles of the pump and harmonic radiation. The latter dependences, especially under conditions of multibeam irradiation, make the diagnostics of the plasma temperature via the harmonic spectrum difficult in the $n_c/4$ region, and necessitate special calculations of the form of the harmonic spectrum, given the conditions for the irradiation and observation, and given the distributions of the velocity and density in the plasma corona. The experimental results were interpreted on the basis of the developed theory.

The authors are grateful to N. N. Demchenko for a discussion of the results of the hydrodynamic calculations for the plasma corona.

[1]N. G. Basov, V. Yu. Bychenkov, O. N. Krokhin *et al.*, Kvant. Elektron. (Moscow) **6**, 1829 (1979) [Sov. J. Quant. Electrona. **9**, 1081 (1979)].
[2]A. I. Avrov, V. Yu. Bychenkov, O. N. Krokhin *et al.*, Pis'ma Zh. Eksp. Teor. Fiz. **24**, 293 (1976) [JETP Lett. **24**, 262 (1976)].
[3]A. I. Avrov, V. Yu. Bychenkov, O. N. Krokhin *et al.*, Zh. Eksp. Teor. Fiz. **72**, 979 (1977) [Sov. Phys. JETP **45**, 507 (1977)].
[4]V. Yu. Bychenkov, V. P. Silin, and V. T. Tikhonchuk, Fiz. Plazmy **3**, 1314 (1977) [Sov. J. Plasma Phys. **3**, 730 (1977)].
[5]V. V. Aleksandrov, S. I. Anisimov, and M. V. Brenner, Zh. Eksp. Teor. Fiz. **71**, 1826 (1976) [Sov. Phys. JETP **44**, 958 (1976)].
[6]H. C. Pant, K. Eidman, P. Sacksenmair, and R. Sigel, Opt. Comm. **16**, 396 (1976).
[7]E. Fabre, C. Carban, C. Popvics *et al.*, Proc. VI Int. Conf. on Plasma Phys. and Contr. Nucl. Fusion Res., Berchtesgaden, 1976, Vol. 2, p. 597.
[8]C. Garban, E. Fabre, C. Stenz *et al.*, J. de Phys. Lett. **39**, 165 (1978).
[9]P. D. Carter, S. M. L. Sims, H. C. Barra, and R. C. Evans, Phys. Rev. Lett. **44**, 1407 (1980).
[10]E. McGoldrick and S. M. L. Sims, Opt. Comm. **39**, 172 (1981).
[11]E. McGoldrick, S. M. L. Sims, R. E. Turner, and O. Willi, *ibid.* **50**, 107 (1984).
[12]V. Aboites, T. P. Hughes, E. McGoldrick *et al.*, Phys. Fluids **28**, 2555 (1985).
[13]L. M. Gorbunov, Yu. S. Kas'yanov, V. V. Korobkin, A. I. Polayanichev, and A. P. Shevelenko, FIAN Preprint No. 126, 1979.
[14]V. Yu. Bychenkov, A. A. Zozulya, Yu. S. Kal'yanov, A. V. Kilpio, and V. T. Tikhonchuk, Zh. Eksp. Teor. Fiz. **84**, 936 (1983) [Sov. Phys. JETP **57**, 544 (1983)].
[15]R. W. Short, W. Seka, K. Tanaka, and A. Williams, Phys. Rev. Lett. **52**, 1496 (1984).
[16]R. E. Turner, D. W. Phillion, B. F. Lasinski, and E. M. Campbell, Phys. Fluids **27**, 511 (1984).
[17]M. C. Richardson, *Laser Interaction and Related Plasma Phenomena*, Vol. 6, Proc. 8 Workshop, Monterey, 1982, p. 903.
[18]K. Tanaka, L. M. Goldman, and W. Seka, Phys. Rev. Lett. **48**, 1179 (1982).
[19]D. M. Villeneuve, R. L. Keck, B. B. Afegan, W. Seka, and E. A. Williams, Phys. Fluids **27**, 721 (1984).
[20]H. Figueroa, C. Joshi, H. Azechi, N. A. Ebrahim, and K. Estabrook, *ibid.* **27**, 187 (1984).
[21]K. A. Tanbaka, B. Boswell, R. S. Craxton *et al.*, Phys. Fluids **29**, 2910 (1985).
[22]A. A. Offenberger, A. Ng, L. Pitt, and M. R. Cervenan, Phys. Rev. **A18**, 746 (1978).
[23]H. A. Baldis and C. J. Walsh, Phys. Fluids **26**, 1364 (1983).
[24]J. Mejer and H. Houtman, *ibid.* **28**, 1549 (1985).
[25]D. M. Villeneuve, H. A. Baldis, and C. J. Walsh, *ibid.* **28**,1545 (1985).
[26]H. C. Barr, Rutherford Lab. Ann. Report NRL-79-036, 1979, Sec. 8.3.3.
[27]E. Z. Gusakov, Pis'ma Zh. Tekh. Fiz. **3**, 1219 (1977) [Sov. J. Tech. Phys. Lett. **3**, 564 (1977)].
[28]A. A. Zozulya and V. P. Silin, Fiz. Plazmy **8**, 859 (1982) [Sov. J. Plasma Phys. **8**, 488 (1982)].
[29]A. A. Zozulya and V. P. Silin, *ibid.* **8**, 1156 (1982) [**8**, 653 (1982)].
[30]V. Yu. Bychenkov, A. A. Zozulya, V. P. Silin, and V. T. Tikhonchuk, Beitr. Plasmaphysik **23**, 331 (1983).
[31]L. V. Krupnova and V. P. Silin, Phys. Plazmy **4**, 867 (1978) [Sov. J. Plasma Phys. **4**, 487 (1978)].
[32]V. A. Roslyakov and A. N. Starostin, Zh. Eksp. Teor. Fiz. **73**, 1747 (1977) [Sov. Phys. JETP **46**, 917 (1977)].
[33]H. C. Barr, J. I. M. Boyd, L. A. T. Cardner, and R. Rankin, Phys. Fluids **27**, 2730 (1984).
[34]Yu. V. Afanas'ev, E. G. Gamalii, N. N. Demchenko, O. N. Krokhin, and V. B. Rozanov, Zh. Eksp. Teor. Fiz. **79**, 837 (1980) [Sov. Phys. JETP **52**, 425 (1980)]. Trudy FIAN **134**, 42 (1982).

Translated by J. G. Adashko